

Primljen / Received: 17.10.2020.

Ispravljen / Corrected: 28.1.2021.

Prihvaćen / Accepted: 25.3.2021.

Dostupno online / Available online: 10.6.2021.

# A simplified fundamental period equation for RC buildings

## Authors:



**Abdullah Yiğit**, M.Sc. CE  
Van Yuzuncu Yil University, Turkey  
Department of Civil Engineering  
[abdullahyigit6521@gmail.com](mailto:abdullahyigit6521@gmail.com)



Assoc.Prof. **Barış Erdil**, PhD. CE  
Van Yuzuncu Yil University, Turkey  
Department of Civil Engineering  
[bariserdil@yyu.edu.tr](mailto:bariserdil@yyu.edu.tr)  
Corresponding author



Assoc. Prof. **İsmail Akkaya**, PhD. CE  
Van Yuzuncu Yil University, Turkey  
Department of Geophysical Engineering  
[iakkaya@yyu.edu.tr](mailto:iakkaya@yyu.edu.tr)

Research Paper

**Abdullah Yiğit, Barış Erdil, İsmail Akkaya**

## A simplified fundamental period equation for RC buildings

Considering the huge differences in the prediction and organization of equations available in the literature, this paper aims at developing a reliable equation including mass and stiffness parameters. Microtremor (ambient vibration) measurements were taken from 23 RC buildings and their fundamental periods were compared to the dynamic analysis results. Building models were then calibrated to account for the infill wall effect. After that, 156 RC buildings were 3D modelled and their dynamic analysis results were used to calibrate the proposed fundamental period equation.

### Key words:

reinforced-concrete building, stiffness, fundamental vibration period, dynamic analysis

Prethodno priopćenje

**Abdullah Yiğit, Barış Erdil, İsmail Akkaya**

## Pojednostavljen izraz procjene osnovnog perioda vibriranja AB građevina

Uzimajući u obzir velike razlike u procijenjenim vrijednostima osnovnog perioda vibriranja i kompleksnost izraza procjene dostupnih u literaturi, ovaj rad usmjeren je na razvijanje pouzdanih izraza procjene koja uključuje parametre mase i krutosti konstrukcije. Uspoređene su vrijednosti osnovnog perioda vibriranja 23 armiranobetonske zgrade određene mjerenjem mikrotremora (ambijentalne vibracije) i dinamičkom analizom. Zatim su računalni modeli zgrada nadograđeni kako bi se obuhvatio efekt ispunskog ziđa. Nakon toga je provedena dinamička analiza prostornih modela 156 armiranobetonskih građevina, čiji su rezultati korišteni za podešavanje predloženog izraza procjene osnovnog perioda vibriranja.

### Ključne riječi:

armiranobetonska građevina, krutost, osnovni period vibriranja, dinamička analiza

Vorherige Mitteilung

**Abdullah Yiğit, Barış Erdil, İsmail Akkaya**

## Vereinfachte Ausweisung der Einschätzung des Grundzeitraums des Vibrierens von Stahlbetongebäuden

Unter Berücksichtigung von großen Unterschieden in den eingeschätzten Werten des Grundzeitraums des Vibrierens, sowie unter Berücksichtigung der Komplexität der Ausdrücke im Hinblick auf die Einschätzung, welche in der Literatur zugänglich sind, ist diese Arbeit auf die Entwicklung von zuverlässigen Ausdrücken der Einschätzung ausgerichtet, welche die Parameter der Masse und der Steifigkeit der Konstruktion umfasst. Es wurden die Werte des Grundzeitraums des Vibrierens von 23 Stahlbetongebäuden verglichen, welche durch die Messung von Mikrovibrationen (Umgebungsvibrationen), sowie durch die dynamische Analyse festgelegt wurden. Danach wurden die Rechnermodelle von Gebäuden angebaut, damit der Effekt einer Ausfüllungswand umfasst werden kann. Danach wurde die dynamische Analyse von Raummodellen von 156 Stahlbetongebäuden durchgeführt, deren Ergebnisse für die Anpassung des vorgeschlagenen Ausdrucks der Einschätzung des Grundzeitraums des Vibrierens genutzt wurden.

### Schlüsselwörter:

Stahlbetongebäude, Steifigkeit, Grundzeitraum des Vibrierens, dynamische Analyse

## 1. Introduction

Seismic design starts from a reliable seismic force, which is directly influenced by vibration periods. Vibration periods on the other hand depend on the mass and stiffness parameters of the buildings. Therefore, it can be said that seismic design is a trial and error procedure in which interaction between the mass, stiffness and seismic capacity should be well established to obtain a reasonable seismic performance. In order to reduce the trial and error procedure, several codes offer a starting point covering the size of the elements, orientation, number of storeys, material properties, etc. Considering these starting parameters, they present natural vibration period equations to calculate the seismic load to be imposed on the building. That natural vibration period is assumed to be the fundamental period of the building, and a great portion of the mass is assumed to contribute to that vibration mode. Although complex equations are available in codes, mainly simpler equations, mostly involving the height of the building or the number of storeys, are encouraged and used to simplify the problem.

It is known that a typical building has several vibrational modes that are influenced by the amount of load carrying and non-load bearing elements, height of the building, number of storeys, plan dimensions, strength of structural material, etc. These parameters contribute to the stiffness and mass of the building. The more the load carrying and non-load bearing elements, the greater the stiffness and thus the lower the periods. Moreover, higher mass results in higher periods. A general relationship between the mass, stiffness, and period is shown in Equation (1). As it can be seen, the mass is proportional to the period, while the stiffness is inversely proportional.

$$T = 2\pi \sqrt{\frac{m}{k}} \quad (1)$$

Several studies have focused on the influence of structural and non-structural parameters on the fundamental period of reinforced concrete buildings. It has been established that the height of the building or the number of storeys have a significant effect on the natural vibration period (shortly period). The greater the height or the number of storeys, the longer the period [1-2]. Since these parameters have been found to be the most important ones, several codes utilize only the height of the building or the number of storeys in their period equations [3-6].

As shear walls are stiffer than columns, shear wall buildings have greater lateral load carrying capacity as compared to frame buildings, which results in the reduction of periods [7-8]. This reduction is related to an increase in lateral stiffness although the mass is slightly increased in shear wall buildings. Even though infill walls are most often assumed to be non-load bearing elements, it has been established that they have great influence on natural vibration periods. Since natural

vibration periods are based on low amplitude vibrations, and as no damage is introduced in infill walls at such vibration regimes, their great in-plane stiffness contributes to lateral stiffness of the building and results in reduced natural vibration periods. Therefore, their contribution to the stiffness should be considered in low amplitude vibrations. However, when the vibration amplitude is increased, it has been established that infill walls, being brittle, actually crack and that their contribution to stiffness reduces significantly [9-11]. Besides, the natural vibration period is also affected by plan dimensions, number of bays and spacing of the bays being related to stiffness of the building. Researchers have established that an increase in spacing of the bays results in longer natural vibration periods. On the other hand, it was found that natural vibration periods slightly shortened when the number of bays increased [12, 2].

The vibration period of a building is affected by the state of damage. If the building is in undamaged state and the vibration amplitude is small, then the period in this state is called the elastic period. However, when a building incurs damage due to vibration forces then, depending on the damage level, the elastic period shifts to inelastic periods, which are longer than elastic periods [7]. It is not easy to determine inelastic periods as they depend on the damage level and damping, which are in turn affected by the level of lateral displacements mainly resulting from earthquake action. Codes only deal with inelastic periods explicitly when the seismic performance is to be determined using nonlinear procedures [13-14, 6]. When the building is designed or checked considering the elastic design spectrum covering general earthquake information of a specified region, then the elastic period will serve the needs and can be used to calculate possible lateral earthquake loads acting on the building. For simplicity reasons, codes mainly deal with elastic periods but somehow they explicitly include the damage state of buildings by utilizing reduced stiffness of the load carrying elements. Therefore, one should never forget that the natural vibration period is not an elastic period, that it includes several assumptions, and that it is affected by several parameters.

Vibration periods of buildings can be measured directly on site using several techniques. The forced vibration equipment exerts a predetermined force on the building, and accelerometers record the accelerations which are correlated to natural vibration periods [15-19]. Since this technique is hard to perform, an alternative technique, i.e. the so called microtremor technique, can also be adopted. In this case, small amplitude ambient vibrations are recorded from the predetermined storeys and the recordings are converted to frequencies and periods. Microtremor technique being easy and cheap, it has been utilized by a number of researchers, and so ample data on this technique are available in the literature [16, 18-22].

In the context of the above information, this study tries to establish a reliable natural vibration period of the low- and

mid-rise reinforced concrete buildings, and takes into account main structural parameters such as the building height, plan dimensions, strength of concrete, and the quantity of load carrying elements and non-load bearing elements. As many parameters are inevitable to develop a complex interaction, the main aim of this study is to simplify the problem and reduce the complexity in the interaction of various parameters. The study considered in this paper is conducted using the following procedure:

- Microtremor measurements were taken from several RC buildings.
- These buildings were 3D modelled using SAP2000 v.20 [23] without considering infill walls, and dynamic analyses were performed to obtain natural vibration periods.
- Buildings were then modelled considering the infill walls, and the analysis results were compared with microtremor measurements.
- Models were calibrated taking into account the infill walls.
- A theoretical equation was developed.
- The equation was compared to the periods from the calibrated models.
- New buildings were modelled, and their periods were compared with the equation.
- Additional calibration of the equation was conducted.
- Several new buildings, other than the previous ones, were modelled and their periods were compared to the equation.
- Comparison between the available studies were conducted.

## 2. Available period equations

Simple equations to calculate natural vibration periods are necessary since it is not always possible to analyse a 3D building, and the lateral seismic force acting on a building should be known before the analysis. Because of this problem, several researchers have proposed simplified equations and codes, or further simplified those equations. Available equations are presented in this section.

Some codes consider the height of the building ( $H$ ) as the main parameter and insert a constant to distinguish the building material. The interaction between the height and the constant differs in various codes. For example, The Building Standard Law of Japan [3] offers Equation (2) and utilizes  $\alpha$  as the constant whose value is equal to zero "0" in RC buildings and "1" in steel buildings. On the other hand, the Uniform Building Code [5] and TEC [6] use the same equation as the one given in Equation (3), and the building material is represented by the  $C_t$  constant. For steel buildings, UBC [5] specifies that  $C_t$  is 0.0853, while it is equal to 0.08 in TEC [6]. As for RC buildings,  $C_t$  is equal to 0.0731 in UBC [5] and amounts to 0.07 in TEC [6].

$$T = (0.02 + 0.01\alpha)H \quad (2)$$

$$T = C_t H^{0.75} \quad (3)$$

However, some codes, like the National Building Code of Canada [4], further simplify the equation and consider only the number of storeys from the ground ( $N$ ), as shown in Equation (4).

$$T = 0,1N \quad (4)$$

In addition to the above code equations, many authors have proposed equations involving only the height of the building, as given in Table 1. Chopra and Goel [24] placed accelerometers on selected buildings and recorded vibrations from the 1971 San Fernando earthquake till the 1994 Northridge earthquake, and then compared the period results with available equations. Upon realizing significant difference between the recorded and calculated periods, they recommended a new equation as given in the table. It is similar to Equation (3) but the constants are different. Hong and Hwang [25] analysed RC frame buildings and, performing regression analysis, they proposed a period equation including the height of the building as given in the table. Crowley and Pinho [26] analysed RC buildings with infill walls using an equivalent analytical procedure and, from dynamic analysis, they proposed a simplified period equation. Guler et.al. [27] developed a period equation for RC buildings with infill walls by performing analytical and experimental approaches. Hatzigeorgiou and Kanapitsas [28] performed a dynamic analysis for 20 distinct real RC buildings to record their natural vibration periods. Having the periods, they performed regression analysis to correlate the height with the periods and finally ended up with an equation similar to Equation 3, as given in Table 1.

**Table 1. Natural vibration period equations**

The study	Period equations
Chopra and Goel [24]	$T = 0.067H^{0.9}$
Hong and Hwang [25]	$T = 0.0294H^{0.804}$
Crowley and Pinho [26]	$T = 0.055H$
Guler et al. [27]	$T = 0.026H^{0.9}$
Hatzigeorgiou and Kanapitsas [28]	$T = 0.075H^{0.75}$

In addition to the previous ones, there are some equations that require several structural parameters of buildings. For example, in the Indian Standard Criteria for Earthquake Resistant Design of Structures [29] the period equation contains  $H$ , and the plan dimension is considered ( $L_i$ ), as shown in Equation (5).

$$T_i = 0.09 \frac{H}{\sqrt{L_i}} \quad (5)$$

Balkaya and Kalkan [30] analysed several shear wall buildings and, considering structural and architectural

parameters, they proposed Equation (6). In the equation,  $J$  is the polar moment of inertia,  $I_{xx}$  is the moment of inertia in x-axis,  $I_{yy}$  is the moment of inertia in y-axis,  $\beta$  is the ratio of long plan dimension to the short one,  $\rho_{ol}$  is the ratio of the shear wall area in short plan direction to the total floor area,  $\rho_{ol}$  is the ratio of the shear wall area in long plan direction to the total floor area,  $\rho_{os}$  is the ratio of the minimum shear wall area to the total floor area and depending on plan shape  $C, b_1, b_2, b_3, b_4, b_5, b_6$  are the constants found from regression analysis.

$$T = Ch^{b_1} \beta^{b_2} \rho_{ol}^{b_3} \rho_{ol}^{b_4} \rho_{os}^{b_5} J^{b_6}, \quad J = I_{xx} + I_{yy} \quad (6)$$

Amanat and Hoque [12], constructed their equation based on Equation (3) and modified it with three structural and non-structural parameters, i.e. spacing of bays ( $A$ ), number of bays ( $B$ ), and percentage of infill walls ( $D$ ), Equation (7).

$$T = ABDC_t H^{3/4} \quad (7)$$

Kose [31] performed a dynamic analysis on 3D models of 189 RC frame buildings to determine their natural vibration periods. After the analysis, he proposed an equation based on  $H$ , number of bays ( $B$ ), frame type ( $F$ , for infilled frames  $F = 1$ , for soft storey frames  $F = 2$  and for bare frames  $F = 3$ ), ratio in percentage of shear walls to the total floor area ( $S$ ), and the area ratio of infill walls to total panels ( $I$ ), Equation (8).

$$T = 0.0935 + 0.0301H + 0.0156B + 0.0039F - 0.1656S - 0.0232I \quad (8)$$

Nyarko et al. [32] have different approach in which the direction considered is important. From 600 analyses of different RC buildings, they performed a nonlinear regression analysis and ended up with Equation (9). In the equation,  $C_1, C_2, C_3$  and  $C_4$  are the constants depending on the direction considered,  $B_x$  and  $B_y$  are the number of bays in the long and short directions, respectively.

$$T = C_1 N^{C_2} + C_3 \left( \frac{B_x}{B_y} \right)^{C_4} \quad (9)$$

Asteris et al. [2] investigated the effect of the number of storeys, number of bays, bay spacing, stiffness of the infill walls ( $E_i$ ), and percentage of the openings ( $a_w$ ) (for frames without infills it is 100 % and for infills without openings it is 0 %), on natural vibration periods of RC buildings. From the results of dynamic analysis, they performed regression analysis and proposed Equation (10).

$$T = (0.55407 + 0.5679\sqrt{H} - 0.00048A - 0.00027a_w - 0.00425E_i + 0.0020\sqrt{HA} + 0.00016\sqrt{Ha_w} - 0.0032\sqrt{HE_i} + 0.00013Aa_w - 0.00017AE_i + 0.00010a_w E_i)^5 \quad (10)$$

It can be observed that, from complex to simple, there are several types of period equations in the literature that predict the natural vibration period of a single RC building differently. As shown in Figure 1 in which 156 RC building data are presented, there is a huge difference between each predicted period. For example, for the 147<sup>th</sup> building, although IS2002 calculates the period as 0.295 s, Crowley and Pinho [26] evaluate it as 1.5 s. Other equations have predictions between these extremes. The actual natural vibration period of this building has been found to be 0.28 s. Considering the huge differences in the predictions, and the organization of the equations available in the literature, which are mainly based on regression analysis, this paper aims at developing a reliable equation including mass and stiffness parameters in a simple manner.

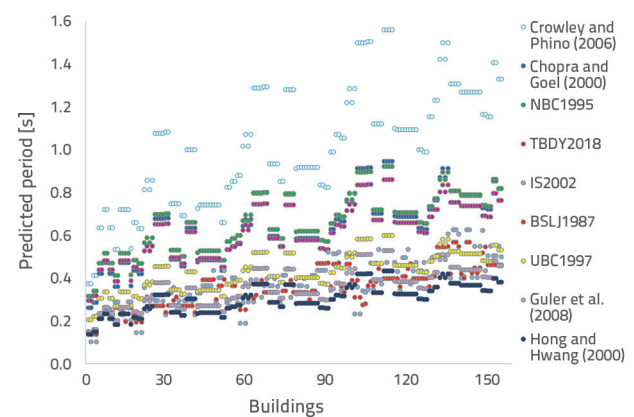


Figure 1. Period prediction in available studies

### 3. Model calibration

Since the aim of this study is to construct a reliable natural vibration period of low and mid-rise RC buildings, several buildings should be studied. Table 2 shows the buildings that were used to calibrate 3D models of the buildings and help to construct the natural vibration period equation. In this table, microtremor (Mcr.) measurements were taken from the first 23 buildings which were utilized in the model calibration process. The remaining 20 buildings were utilized, together with the previous 23 buildings, in the calibration of the natural vibration period equation. Figure 2 shows the buildings from which microtremor readings were recorded.

Buildings used in the model calibration process are situated in Van City, which is located in the eastern part of Turkey, and their properties are all different. They experienced the 2011 Van Earthquakes,  $M_w = 7.1$  on 23 October, and  $M_w = 5.6$  on 9 November [33-34]. The concerned buildings have 2 and 5 storeys. In addition, the concrete strength ( $f_c$ ) varies from 8 to 25 MPa, average being 11.9 MPa, which is well below the minimum  $f_c$  specified in Turkish Earthquake Codes (TEC) (in TEC1975 and TEC1997  $f_{c,min} = 18$  MPa, in TEC2007  $f_{c,min} = 20$  MPa and in TEC2018  $f_{c,min} = 25$  MPa). Although the buildings were built after 1980, most of them exhibit low strength. Plan

Table 2. Building properties used to calibrate the proposed equation

Bldg. No	H [m]	N	$f_c$ [MPa]	$L_x$ [m <sup>2</sup> ]	$L_y$ [m <sup>2</sup> ]	$A_{cx}$ [m <sup>2</sup> ]	$A_{cy}$ [m <sup>2</sup> ]	$A_{swx}$ [m <sup>2</sup> ]	$A_{swy}$ [m <sup>2</sup> ]	$A_{mwx}$ [m <sup>2</sup> ]	$A_{mwy}$ [m <sup>2</sup> ]	Mcr.
A1	14.8	4	12	24.9	14.0	3.0	4.7	5.7	7.7	7.2	6.2	YES
A2	15.6	4	11	43.2	32.0	10.0	9.9	15.8	18.9	7.9	5.7	YES
A3	13.5	4	13	17.5	17.0	2.8	0.4	4.9	4.4	2.4	5.2	YES
A4	13.5	4	18	14.3	16.2	1.0	2.9	2.2	2.5	0.9	8.5	YES
A5	13.5	4	15	34.3	17.0	4.9	0.7	9.8	8.8	3.5	4.0	YES
A6	13.5	4	19	17.5	17.0	2.8	0.4	4.9	4.4	2.4	5.2	YES
A7	13.5	4	13	14.3	16.2	1.0	2.9	2.2	2.5	0.9	8.5	YES
A8	13.5	4	15	34.8	17.3	4.9	0.7	9.8	8.8	3.5	4.0	YES
A9	11.6	3	11	33.9	23.4	4.5	5.7	14.4	12.3	2.7	2.0	YES
A10	11.6	3	10	39.9	23.4	4.5	5.7	14.4	12.3	1.4	3.9	YES
A11	13.1	3	11	33.9	23.4	4.5	5.7	14.4	12.3	2.7	2.0	YES
A12	13.1	3	13	39.9	23.4	4.5	5.7	14.4	12.3	1.4	3.9	YES
A13	11.6	3	25	48.3	16.5	6.5	5.5	7.0	10.5	12.7	9.8	YES
A14	12.0	3	10	36.4	22.4	2.6	5.0	15.1	15.7	9.8	3.8	YES
A15	12.0	4	14	52.5	22.4	3.5	9.7	18.7	18.7	6.8	5.9	YES
A16	15.2	5	11	52.5	22.4	3.5	9.7	18.7	18.7	9.8	7.1	YES
A17	7.5	2	14	28.0	24.0	3.2	2.2	4.4	7.9	8.9	10.2	YES
A18	13.6	4	9	28.2	13.7	4.4	3.1	5.1	7.0	2.1	10.7	YES
A19	13.6	4	10	28.2	13.7	4.4	3.1	5.1	7.0	10.7	2.1	YES
A20	16.0	5	11	13.5	20.4	1.8	3.7	4.6	2.8	1.3	4.3	YES
A21	6.8	2	9	36.0	36.0	6.8	9.7	7.1	7.7	13.6	11.3	YES
A22	13.1	3	11	33.0	16.7	0.2	10.4	7.9	9.0	4.2	5.3	YES
A23	13.1	3	9	33.0	16.7	0.2	10.4	7.9	9.0	4.2	3.5	YES
A24	14.8	4	12	24.9	14.0	3.0	4.7	2.6	4.8	10.3	9.2	---
A25	15.6	4	11	43.2	32.0	5.0	6.6	4.2	8.7	13.9	8.8	---
A26	23.6	5	25	48.3	16.5	6.5	5.5	0.9	6.2	16.3	12.5	---
A27	13.5	4	18	14.3	16.2	1.0	2.9	0.0	1.3	1.8	9.1	---
A28	18.2	4	11	33.0	16.7	0.2	10.4	4.8	2.3	4.2	10.2	---
A29	18.2	4	9	33.0	16.7	0.2	10.4	4.8	2.3	4.2	10.2	---
A30	13.5	4	13	14.3	16.2	1.0	2.9	0.0	1.3	1.8	9.1	---
A31	12.0	4	10	36.4	22.4	2.6	5.0	12.2	9.7	12.7	11.1	---
A32	11.6	3	25	48.3	16.5	6.5	5.5	0.9	6.2	16.3	12.5	---
A33	12.0	3	10	36.4	22.4	2.6	5.0	12.2	9.7	12.7	11.1	---
A34	12.0	4	14	52.5	22.4	3.5	9.7	11.7	12.7	13.4	6.8	---
A35	15.2	5	11	52.5	22.4	3.5	9.7	11.7	12.7	16.4	8.0	---
A36	7.5	2	14	28.0	24.0	3.2	2.2	2.7	1.7	10.6	16.4	---
A37	13.6	4	9	28.2	13.7	4.4	3.1	1.6	3.0	3.9	14.0	---
A38	13.6	4	10	28.2	13.7	4.4	3.1	1.6	3.0	12.4	5.4	---
A39	9.8	3	8	31.2	19.5	2.9	2.7	0.8	4.1	7.8	12.7	---
A40	16.0	5	11	13.5	20.4	1.8	3.7	0.7	2.8	3.9	4.3	---
A41	6.8	2	9	36.0	36.0	6.8	9.7	3.7	4.7	13.6	12.3	---
A42	13.1	3	11	33.0	16.7	0.2	10.4	4.8	2.3	4.2	10.2	---
A43	13.1	3	9	33.0	16.7	0.2	10.4	4.8	2.3	4.2	10.2	---

dimensions ( $L_x$  and  $L_y$ , longer and shorter dimensions in plan, respectively) are also different and building plans vary from square to rectangular. As for the load carrying vertical members,  $A_{cx}$ ,  $A_{cy}$  stand for the total column area in x and y directions at ground floor, respectively,  $A_{swx}$ ,  $A_{swy}$  show the total shear wall area in x and y directions at ground floor, respectively,  $A_{mwx}$ ,  $A_{mwy}$  depict the total infill wall area in x and y directions at ground

floor, respectively. While calculating the total infill wall area, the door and window openings were subtracted. The values given in the table were the net infill wall areas. All of the buildings have columns located in x and y directions. However, in some buildings (A3, A4, A5, A6, A7, A8, A22, A23, A42, A43), most of the columns are mainly oriented in one direction. An attempt was made to counter the negative effect of this orientation



Figure 2. Investigated buildings in model calibration

choice via the shear wall, since, in general, buildings have quite a big number of shear walls in two orthogonal directions, except for A16, A27, A30, A32, A39 and A40.

All the buildings given in Table 2 experienced the 2011 Van Earthquakes, and minor damage to their structural and nonstructural elements was observed. Although light damage was registered, most of the buildings were strengthened either globally or locally. In the global strengthening, shear walls were added at certain locations. As for the local strengthening, concrete jackets were applied to the columns, and beams were strengthened using the FRP material. Microtremor measurements were recorded from the strengthened building and the properties given in the table were collected after strengthening except for concrete strength, which indicates the as built concrete quality before strengthening because the amount of additional shear walls and concrete jacketing is low compared to the available structural elements, and contribution of their concrete strength (25 MPa) to the stiffness is limited.

### 3.1. Building models without infill wall effect

As previously noted, the first 23 buildings were used in model calibration because microtremor measurements were taken from these ones only. All the buildings were 3D modelled using SAP2000 v20. Columns and beams were modelled by frame elements whereas area elements were used to model slabs and shear walls. Relevant stiffness modifications were made since TEC2018 [6] states that stiffness of structural members should

be modified under seismic action to account for the cracked section behaviour. For example, bending stiffness values of columns and beams were reduced by 30 % and 65 %, respectively. As for slabs and shear walls, the effective bending stiffness was assumed to be 25 % of the initial stiffness. Columns and shear walls were assumed to have fixed supports at the base. The mass was defined as the sum of dead loads and a portion of live loads. The live load participation is set to 60 % for school buildings and 30 % for residential buildings in TEC2018 [6]. Slabs and shear walls were meshed by 1 x 1 m to provide for mass distribution over the area elements. The dead and live load values were taken from TS498 [35]. The infill wall stiffness was not accounted for in this step. Instead, these values were converted to loads distributed over the beams considering the openings.

Dynamic analyses were performed for the concerned 23 buildings, and natural vibration periods corresponding to the principal axis of the buildings were obtained. The maximum period is selected and compared with the periods extracted from microtremor measurements as shown in Figure 3. As can be seen from the figure, periods from dynamic analysis were longer for most of the buildings. Since the mass of the building is almost constant, the problem indicates that building stiffness values are not that small, and they should be increased considering the infill walls since microtremor readings were recorded from the actual buildings having infill walls, and these infill walls contributed to the stiffness in small amplitude vibrations. Therefore, all the buildings were remodelled considering the stiffness effect of infill walls.

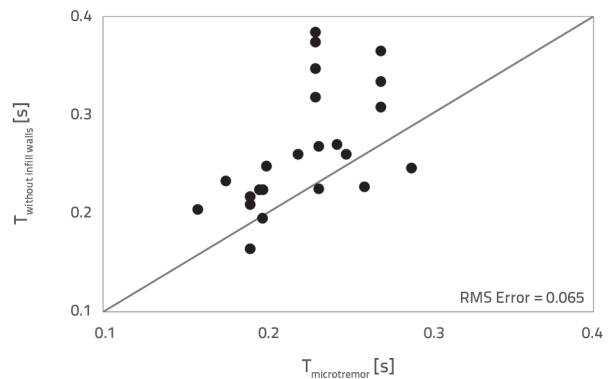


Figure 3. Comparison between periods from microtremor recordings and dynamic analysis

### 3.2. Building models with infill wall effect

Infill walls have significant effect on the overall stiffness of buildings. Micro and macro modelling strategies can be utilized to consider their effects. In the micro modelling approach, finite element methods are used to model the infill walls, whereas in the macro modelling approach infill walls are assumed to be equivalent struts (Figure 4). Polyakov [36] was the first to introduce the equivalent struts with pin ends, and his approach was considered in all the building models covered in this paper. The main parameter in this approach is the effective width of the wall ( $W_m$ ). Several researchers have studied the effective width of walls and proposed a number of relationships [37-46]. Being practical and resulting in average values, the recommendations by Paulay and Priestley [43] for effective width of walls - as given in Equation (11) - were followed in this study.

$$W_m = 0.25D_m \text{ where } D_m^2 = H_m^2 + L_m^2 \tag{11}$$

where  $H_m$  is the height and  $L_m$  is the length of the infill wall.

Another important parameter affecting wall stiffness is the modulus of elasticity ( $E_m$ ) of the infill wall. FEMA 356 [13] was utilized for this purpose and it is assumed that, in fair conditions, compressive strength of masonry can be 4.13 MPa, and that the modulus of elasticity can be found using Equation (12).

$$E_m = 550 f_m \tag{12}$$

It is known that wall stiffness reduces in the case openings are present. Bertoldi et. al. [47] recommended to use the ratio of opening area to infill wall area ( $A_o$ ) and length of the opening to infill wall length ( $A_e$ ) (Equation (13)). The equation was further simplified by Crowley and Pinho [26] and with  $A_o = 20\%$  and  $A_e = 25\%$ , the reduction coefficient for openings ( $r_{ac}$ ) turned out to be approximately 0.4.

$$r_{ac} = 0.78e^{-0.322 \ln A_o} + 0.93e^{-0.762 \ln A_e} \tag{13}$$

While modelling infill walls as equivalent struts, their mass should also be taken into account. For this reason, all the 23 buildings having microtremor readings were remodelled

with equivalent struts considering infill wall openings. After performing dynamic analysis, natural vibration periods were obtained, and they were compared with the microtremor results, as shown in Figure 7. It was established that natural vibration periods shortened significantly since infill walls added stiffness to the buildings, and they got closer to the microtremor results.

By comparing Figure 3 and Figure 5, it can be seen that maximum difference ( $T_{\text{microtremor}}/T_{\text{model}}$ ) reduces from 40% to 30% with the infill wall modelling (Table 2). A similar decrease is also seen in RMS and MS errors. The reduction in RMS error is 55% whereas it is 80% in MS error. Therefore, it can be said that the stiffness and mass of infill walls should be considered in the models.

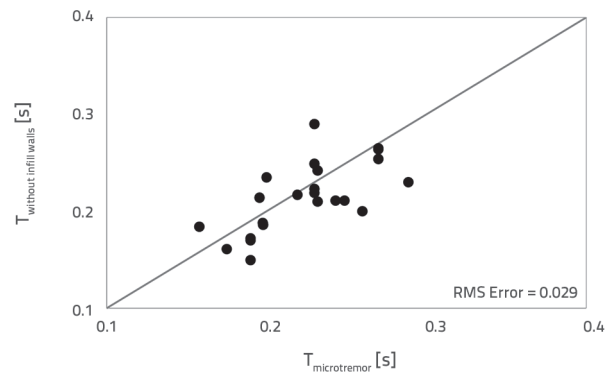


Figure 5. Comparison between periods from microtremor recordings and dynamic analysis of buildings with infill wall effect

Table 3. Errors in the models

Errors \ Models	RMS Error	MS Error	Maximum difference	St. Dev. of difference
Building models without infills	0.0654	0.0034	40 %	16 %
Building models with infills	0.0292	0.0007	30 %	13 %

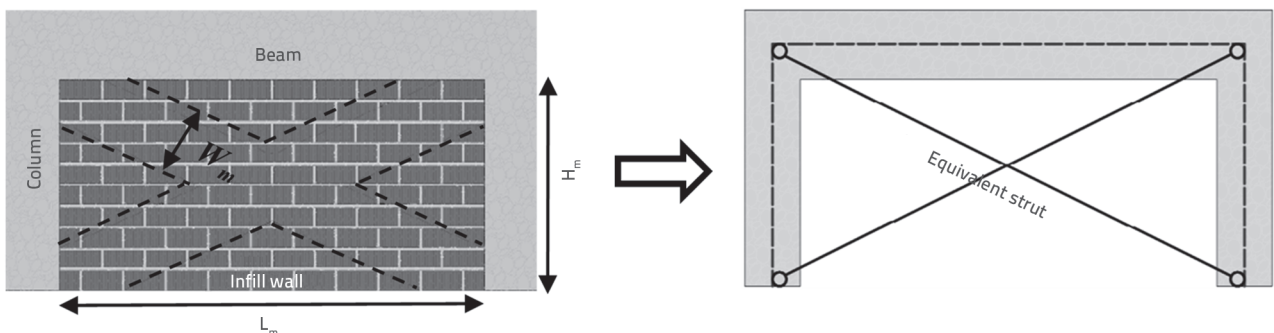


Figure 4. Equivalent strut model of infills

### 4. Developing natural vibration period equation

As previously noted, and as it is well known, the period of a structure is affected by its mass and stiffness, which is formulized as in Equation (1). This equation will be the starting point of this study. Having mass (*m*) and stiffness (*k*), an RC building can be represented by a SDOF system with the equivalent lumped mass (*m*) and equivalent stiffness (*k*), as shown in Figure 6.

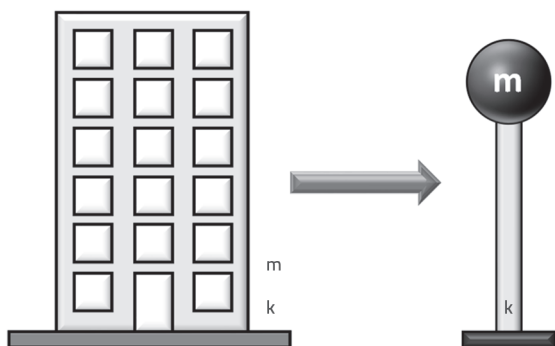


Figure 6. Equivalent cantilever column

The equivalent mass of the building, including dead load and live load, can be calculated from Equation 14 considering the total mass by assuming 1.2 t/m<sup>2</sup> over the entire floors [33]. In the equation, *N* is the number of floors and *A<sub>f</sub>* is the floor area.

$$m = 1.2NA_f \tag{14}$$

The lateral displacement profile of an RC building is affected by several factors: height, lateral load carrying members, and plan area. As stated in ATC40 for the Capacity Spectrum Method, buildings can be categorized into four groups with regard to their lateral displacement profile:

- shear wall buildings
- buildings of equal stiffness
- frame buildings
- buildings with a soft/weak storey.

In all the buildings, although top displacement is the greatest one, the main difference is seen in the lower storeys: although the interstorey lateral displacement is low in shear wall buildings when compared to other storeys, it is much greater in buildings with a soft/weak storey.

In this study, an RC building is assumed to behave like a cantilever column with equivalent stiffness (*k*) whose lateral displacement profile resembles a shear wall building, as given in ATC40 [14]. For the starting point, the equivalent stiffness is assumed to be calculated as given in Equation (15). In the equation, *E* is the modulus of elasticity of concrete, *I* is the moment of inertia of the load carrying members, and *H* is the total height of the building. By implementing the equivalent mass and stiffness, the general equation assumes the form of Equation (16).

$$k = \frac{3EI}{H^3} \tag{15}$$

$$T = 2\pi \sqrt{\frac{1.2NA_f}{\frac{3EI}{H^3}}} \tag{16}$$

Most RC buildings do not behave like a cantilever column; therefore, their equivalent stiffness should be modified. The modification can be done through moment of inertia and height as material properties cannot be changed. In other words, the elastic modulus of concrete is equal to (MEU Law No:6306 [48]). Since the equivalent lateral seismic load is assumed to act like an inverted triangular pattern, and the centre of this triangle is located at 0.67H above the ground, an equivalent height is assumed to be equal to 0.7H because only the first mode behaviour is considered in this study and lateral displacements are assumed to increase with height. As for the moment of inertia, firstly, the building is assumed to be like a rectangular section and then this section is modified through the ratio of the lateral load carrying members (*A<sub>l</sub>*) to the floor area (*A<sub>f</sub>* = *L<sub>j</sub>L<sub>i</sub>*), as given in Equation (17) where *i* and *j* are the principal axes of the building. In the equation, *L<sub>i</sub>* is the long and *L<sub>j</sub>* is the short plan dimension of the building [49]. *A<sub>ti</sub>* is the total area of the shear walls (*A<sub>swi</sub>*), columns (*A<sub>ci</sub>*) and only the 10 % of the infill walls without voids (*A<sub>wi</sub>*) at the ground floor. By adding these terms, the period equation assumes the form given in Equation (19).

$$I_j = \frac{1}{12} [L_j L_i^3] \frac{A_t}{A_f} \tag{17}$$

$$A_{ti} = A_{ci} + A_{swi} + 0.1A_{wi} \tag{18}$$

$$T_i = 2\pi \sqrt{\frac{1.2NL_i L_j}{3 * 5000 \sqrt{f_c} \frac{1}{12} [L_j L_i^3] \frac{A_t}{L_i L_j} \frac{1}{(0.7H)^3}}} \tag{19}$$

Rearranging Equation (19) we end up with Equation (20).

$$T_i = 0.114 \sqrt{\frac{NH^3 L_j}{A_t L_i \sqrt{f_c}}} \tag{20}$$

Periods for each principal axis of the building are calculated and compared with the periods found from dynamic analysis considering the infill wall effect. Figure 7 shows the plan view and photos of the buildings and their structural model with infill walls. After the earlier described model calibration, 43 buildings were modelled, and dynamic analysis was performed. These 43 buildings were replicated either by deleting the top storey to have a reduced storey, or by adding one or two storeys to have a greater number of storeys. By this modification, a total of 156 buildings were obtained and the Equation 20 was verified using these data.

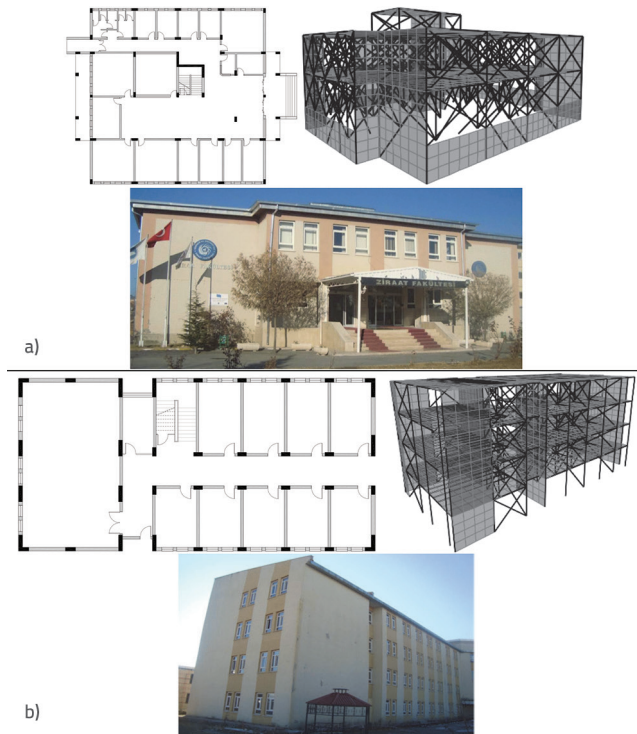


Figure 7. Typical building plans and 3D models: a) Building A17; b) Building A18

Comparison between the periods calculated from Equation (20) and periods obtained from dynamic analysis is given in Figure 8.a. As can be seen, Equation (20) overestimates the periods, and the RMS error is 1.50. Therefore, it is obvious that further calibration is necessary for the equation. In order to further calibrate the equation, the number of storeys and height of the building, being correlated with each other, are combined, while the constant outside the square root and the power of the root are considered to be the main variables  $\gamma$  and  $\beta$ , respectively (Equation (21)). Based on regression analysis,  $\gamma$  and  $\beta$  constants are found to be 0.08 and 0.25, respectively. With these constants, periods are recalculated and compared to the results of dynamic analysis, as shown in Figure 8.b. The RMS error is in this case reduced to 0.048, and it can be seen from

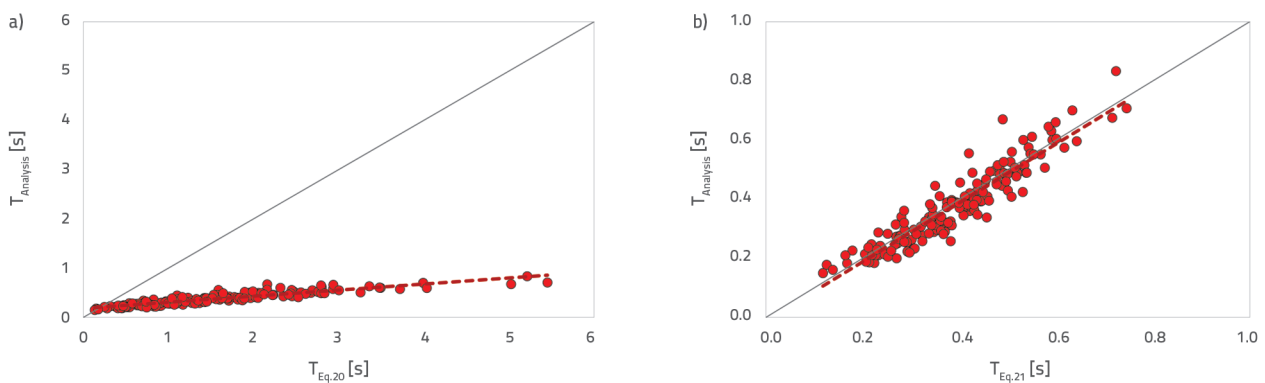


Figure 8. Comparison between the periods from the equations and analysis: a)  $T_{Eq,20}$  versus  $T_{analysis}$  ( $\gamma = 0,114, \beta = 0,5$ ); b)  $T_{Eq,21}$  versus  $T_{analysis}$  ( $\gamma = 0,08, \beta = 0,25$ )

the figure that the predicted periods accumulated at the line of symmetry. The detailed error calculations are summarized in Table 3. It can be seen that the errors were minimized with the new constants, and that dynamic analysis results can be predicted within a reasonable error range.

$$T_i = \gamma H \left[ \frac{L_j}{A_t L_i \sqrt{f_c}} \right]^\beta \quad (21)$$

The final version is obtained as given in Equation (22).

$$T_i = 0.08 H \left[ \frac{L_j}{A_{ti} L_i \sqrt{f_c}} \right]^{0.25} \quad (22)$$

where  $H$  (m),  $L_i$  (m),  $L_j$  (m),  $A_{ti}$  (m<sup>2</sup>) and  $f_c$  (t/m<sup>2</sup>) are the only variables..

Table 4. Errors in the equations

	RMS Error	MS Error	Maximum difference	Dev. of difference
$\gamma = 0,114, \beta = 0,5$	1,468	2,155	671 %	30 %
$\gamma = 0,084, \beta = 0,25$	0,049	0,002	48 %	14 %

The equation indicates that the period is linearly proportional to the height of the building (Figure 9.a), nonlinearly proportional to the ratio of the perpendicular plan dimension to plan dimension of the building parallel to the direction considered (Figure 9.b), and inversely nonlinearly proportional to the concrete strength (Figure 9.c) and area of vertical load carrying members (Figure 9.d). The figures clearly show that  $H$  is the most effective parameter in the equation because with its cubic power, the height affects the stiffness of the structure significantly. Following that,  $A_t$  also affects the stiffness of the structure but, since it uses plan dimensions of structural elements, its effect is not as significant as that of the height, and its influence reduces with the decrease in height. Although  $f_c$  and  $L_j/L_i$  have little influence on the period, they become more effective with an increase in height.

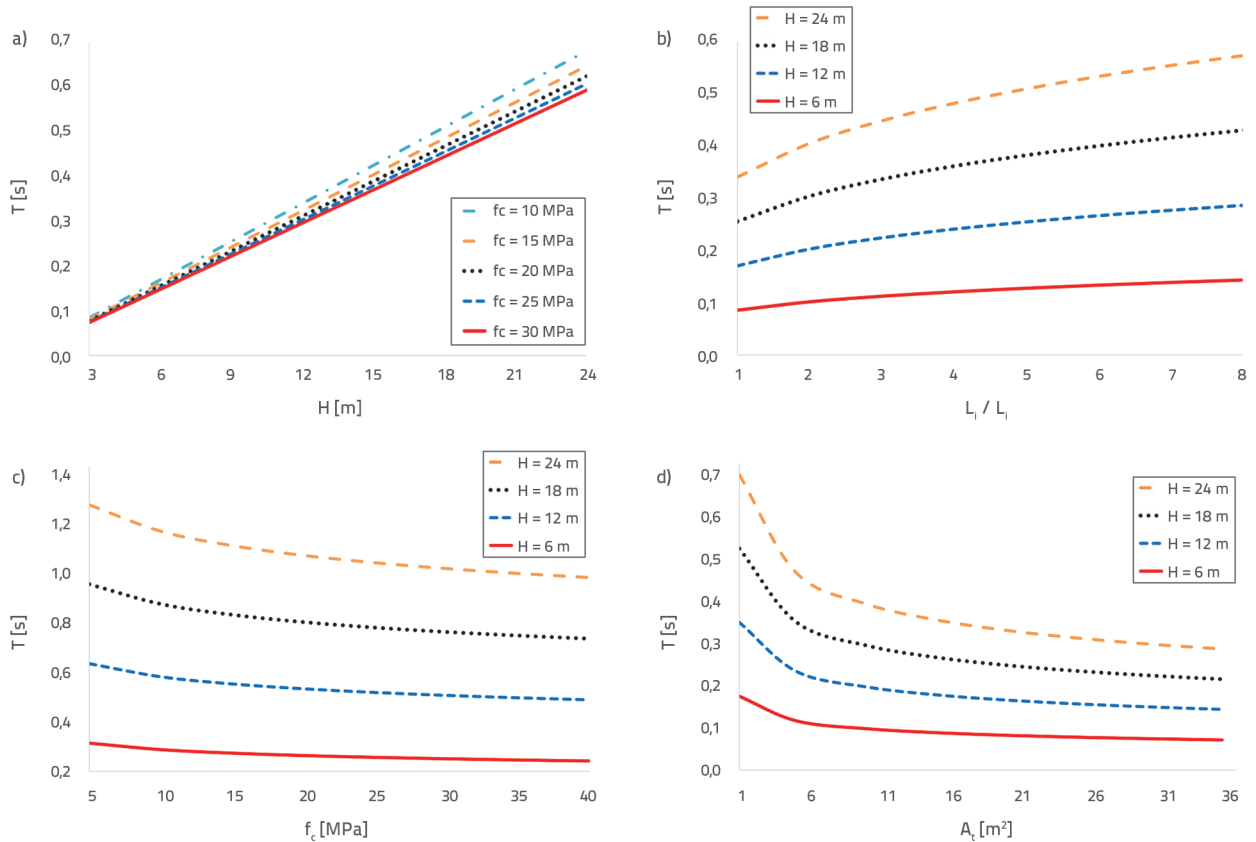


Figure 9. Effect of: a)  $H$ ; b)  $L_x/L_y$ ; c)  $f_c$ ; d)  $A_t$  on period

## 5. Discussion

### 5.1. Verification of the equation

Fifteen different buildings were taken into account (Table 4) in order to verify reliability of the proposed equation (Equation (22)).

The buildings are located at various sites in Turkey: Van, Bingöl and Afyon [33, 50]. Eight buildings from the table experienced Bingöl earthquake on May 1, 2003 with a magnitude of  $M_w = 6.4$ . Besides, two buildings are in Afyon and they were hit by an earthquake of magnitude  $M_w = 6.2$  on February 3, 2002. The remaining five buildings are in Van City. Some of the buildings

Table 5. Building properties used to check the proposed equation

Bldg. No	H [m]	N	$f_c$ [MPa]	$L_x$ [m <sup>2</sup> ]	$L_y$ [m <sup>2</sup> ]	$A_{cx}$ [m <sup>2</sup> ]	$A_{cy}$ [m <sup>2</sup> ]	$A_{swx}$ [m <sup>2</sup> ]	$A_{swy}$ [m <sup>2</sup> ]	$A_{mwx}$ [m <sup>2</sup> ]	$A_{mwy}$ [m <sup>2</sup> ]
B1	13.8	5	13	24.3	13.2	1.3	3.0	4.0	8.2	3.2	12.8
B2	23.3	8	16	21.4	16.9	1.6	4.5	0.4	2.9	4.0	6.8
B3	21.5	7	6	21.0	13.7	0.3	7.8	0.3	0.6	3.9	9.0
B4	21.0	7	8	22.4	26.9	3.5	4.7	0.4	1.0	6.2	14.4
B5	14.0	5	12	14.9	14.3	1.3	3.3	4.4	4.0	4.3	1.8
B6	13.8	5	10	23.1	25.1	6.5	1.4	0.0	2.8	8.9	6.0
B7	15.0	5	10	20.7	10.6	2.1	3.1	0.0	6.6	3.7	3.2
B8	20.4	6	10	37.7	16.8	0.0	5.3	1.4	0.7	0.0	8.0
B9	13.6	4	10	34.5	14.1	0.7	5.1	0.0	0.0	0.0	13.2
B10	13.6	4	15	15.9	12.5	1.9	1.4	3.8	1.2	0.0	1.5
B11	14.0	5	13	21.0	20.0	3.9	4.6	0.0	0.0	2.9	6.1
B12	14.0	5	12	20.6	21.5	2.5	2.6	0.0	1.1	6.1	8.2
B13	11.8	4	15	22.2	23.3	2.4	4.5	0.0	0.0	3.3	14.9
B14	11.9	4	11	29.7	23.7	0.4	10.1	0.0	0.0	1.2	11.5
B15	19.2	6	12	25.2	31.3	1.3	12.7	0.0	0.0	4.7	16.7

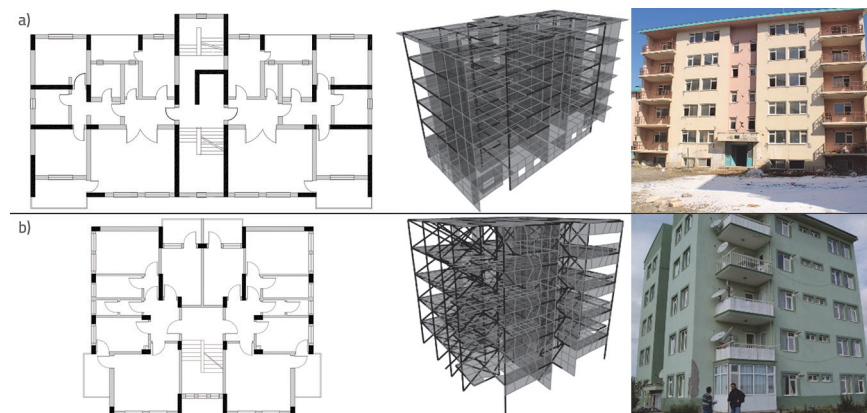


Figure 10. Typical building photos, plans and 3D models given in Table 4: a) Building B1; b) Building B5

given in the table were replicated by adding or removing one storey. Since load carrying members were adversely affected by storey addition, some buildings were not reproduced. Finally, twenty more buildings were reproduced and a total of 35 buildings were utilized at the reliability phase. The maximum number of storeys was kept at 8 and concrete strength varied from 6 to 16 MPa. Some buildings do not have shear walls in either direction. All buildings were again 3D modelled considering the infill wall effect as described above. Representative models are given in Figure 10.

The comparison between predicted periods and analysis periods is shown in Figure 11. As can be seen, the correlation is great, the error is too small, and RMS error is calculated as 0.033. It is also obvious that all data accumulate at the line of symmetry. Therefore, it can be said that the proposed equation has good predictions considering the buildings in Table 4.

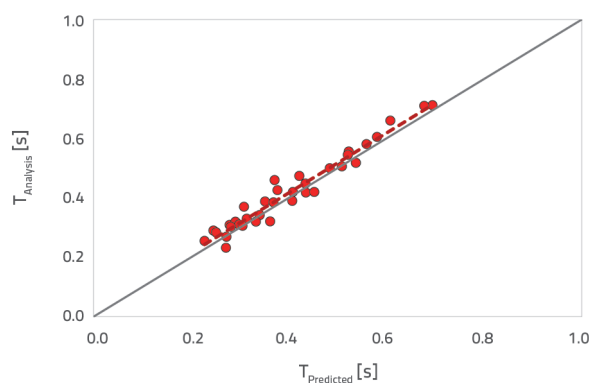


Figure 11.  $T$  from Equation (22) ( $T_{\text{Predicted}}$  versus  $T_{\text{Analysis}}$ )

## 5.2. Comparison with the equations proposed by literature

Analysis results for 35 buildings derived from 15 buildings given in Table 4 were compared to the periods calculated from available equations proposed by researchers [2, 12, 24–28, 31–32] (Figure

12). To simplify the figure, only the trend lines are provided. The figure first indicates that researchers predict the periods differently because they propose different equations. Second, although some researchers [2, 12, 25, 27] predict shorter periods, others predict longer periods as compared to the analysis periods. Most authors predict periods close to the line of symmetry at low periods but the difference from the line of symmetry increases when the period increases. The trend lines of Amanat and Hoque [12] and Asteris et. al. [2] differ from those presented by other authors because they both cross and are close to the line of symmetry. On the other hand, the proposed equation seems to have the best predictions since its trend line is almost on the line of symmetry.

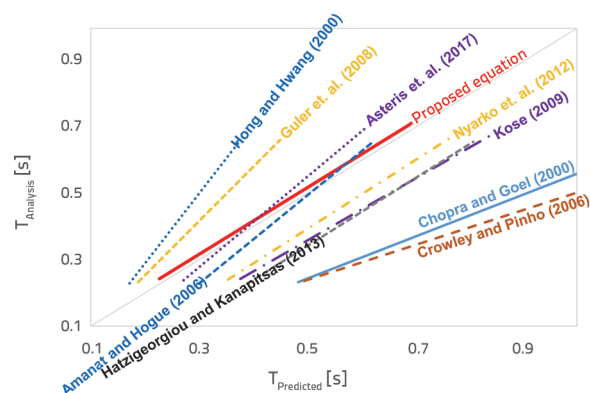


Figure 12. Comparison between analysis periods and periods from equations given in literature

In order to further explore the success of the equations, several errors were calculated as indicated in Table 5. In the table, RMS and MS errors show cumulative errors, and the standard deviation of difference indicates how predictions accumulated over the trend lines. It can be seen from the table that the proposed equation has the lowest RMS and MS errors. Moreover, the maximum difference and the standard deviation of difference are also the lowest. This is followed by the equation proposed by Asteris et. al. [2]. However, in this case, the RMS error is almost two times greater and the MS error is four times greater, compared to the proposed equation. Amanat and Hoque [12] have similar error statistics. Since these two studies consider the spacing and the number of bays, as well as the effect of infill walls, their predictions were found to be close to the analysis results. On the other hand, other researchers' predictions seem to have big errors since they mostly consider the height of the building. Although Kose [31] and Nyarko et. al. [32] consider similar parameters as Amanat and Hoque [12] and Asteris et. al. [2], the relationship

Table 6. Errors and differences in equations presented in literature

Periods (literature)	RMS Error	MS Error	Maximum difference [%]	St. Dev. of difference [%]
Proposed equation	0.033	0.001	19.4	7.8
Asteris et al. [2]	0.063	0.004	28.5	13.2
Amanat and Hoque [12]	0.067	0.004	42.2	16.2
Nyarko et al. [32]	0.128	0.016	70.1	22.2
Guler et al. [27]	0.137	0.019	43.6	9.8
Kose [31]	0.155	0.024	73.8	18.1
Hatzigeorgiou and Kanapitsas [28]	0.166	0.028	84.5	21.0
Hong and Hwang [25]	0.177	0.031	51.3	9.1
Chopra and Goel [24]	0.368	0.136	133.5	25.3
Crowley and Pinho [26]	0.437	0.191	145.4	26.2

between these parameters seems to be weak concerning the building properties given in Table 4. Considering all the data given in Table 5, it can be said that period equations based solely on the height or the number of storeys result in substantial errors.

### 5.3. Comparison with equations presented in codes

The above given results for the same buildings were compared with period predictions using equations presented in codes (Figure 13). As can be seen from the figure, none of the periods calculated from equations given in codes accumulated near the line of symmetry. BSLJ1987 [3] and IS2002 [29] predicted low periods whereas NBCC1995 [4], UBC1997 [5] and TEC2018 [6] predicted high periods as compared to the analysis results. Since the codes only use H (except for IS2002 [29] which uses plan dimension as well), the equations they present are simple, but the errors are high, as given in Table 6, when compared to the ones calculated in Table 4. The best predictions with reasonable errors are given in NRCC1995 [4]. On the other hand, once again, the proposed equation has the best predictions with lower error.

In addition to errors, the dispersion of the period results should also be considered. This dispersion is expressed through standard deviation as given in Table 6. As can be seen, the proposed equation has less dispersion around its trend line given in Figure 13. It is followed by BSLJ1987 [3] but, although it has lower dispersion, its error is great. Other four codes have 20 % dispersion around their trend lines. Therefore, to have a

reliable and better predictions, proposed equations should result in lower error and have lower dispersions.

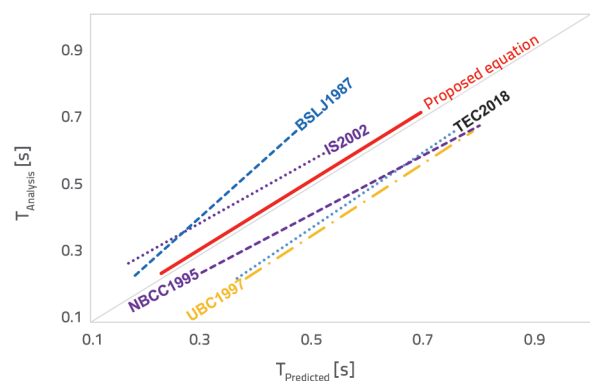


Figure 13. Comparison between analysis periods and periods from equations given in codes

### 5.4 Comparisons considering building properties and analysis results available in literature

The decision was made to make another comparison through the data available in the literature. 144 data containing building properties and dynamic analysis results were compiled [28, 30, 51-58]. The height of the buildings varies between 2 and 14 and building type varies from frame to shear wall buildings. In order to understand the limit of the proposed equation, building properties totally different from the ones used previously in this paper were selected. Analysis results were taken as they are, i.e.

Table 7. Errors and differences in equations given in codes

Periods (literature)	RMS Error	MS Error	Maximum difference [%]	St. Dev. of difference [%]
Proposed equation	0.033	0.001	19.4	7.8
NBCC1995 [4]	0.110	0.012	61.8	19.9
IS2002 [29]	0.129	0.017	47.5	20.1
BSLJ1987 [3]	0.131	0.017	43.2	9.5
TEC2018 [6]	0.131	0.017	72.2	19.6
UBC1997 [5]	0.153	0.023	79.8	20.5

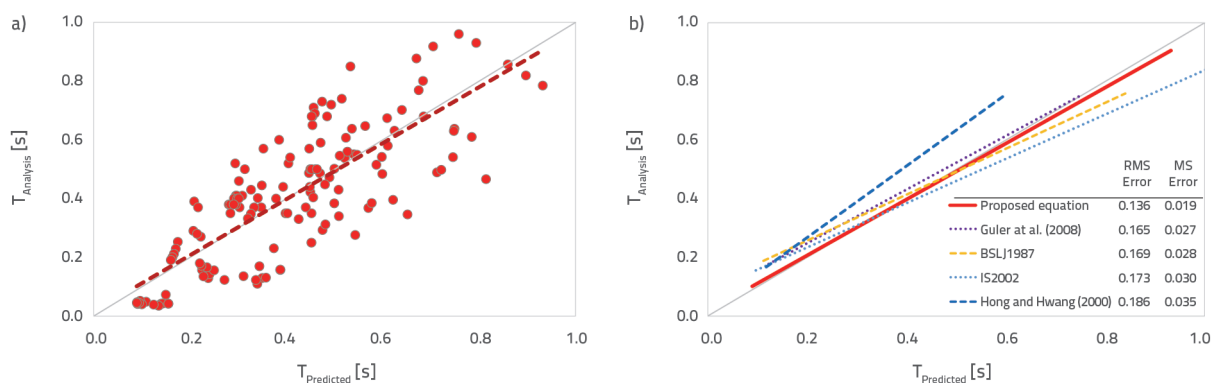


Figure 14. Comparison between analysis periods given in literature and periods from a) proposed equation b) equations presented in codes and literature

no modification was made and no additional dynamic analysis were performed, i.e. period results were taken directly from the literature. The comparison between the periods calculated using Equation 22 and the ones taken directly from the literature as  $T_{\text{Analysis}}$  is given in Figure 14.a. As can be seen, the trend line is almost on the line of symmetry and the dispersion of data is not excessive. The other comparison was made considering the best predictions as seen in Figure 14.b. All available period equations were studied but, to simplify the figures, only the best predictions were presented. Guler et al. [27], BSLJ1987 [3], IS2002 [29], Hong and Hwang [25] have RMS error lower than 0.2. All equations seem to have good predictions, but the RMS error of the proposed equation is again lower compared to other predictions.

### 5.5. Comparison with microtremor measurements

In Figure 15, predictions from Equation 22 are compared with microtremor measurements given in Table 1. The proposed equation seems to result in longer periods but most of the data are accumulated around the line of symmetry. The calculated RMS error is 0.045 and MS error is found to be 0.002. The errors are still reasonable, and predictions are close to microtremor records.

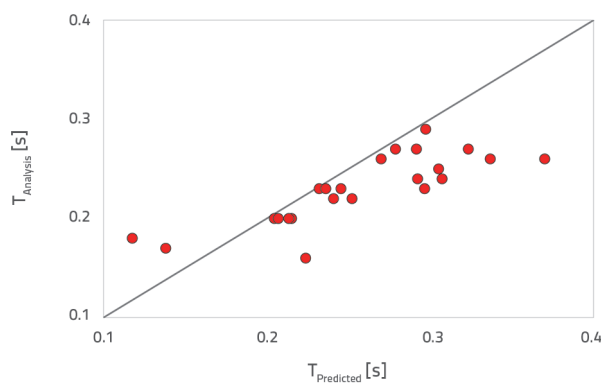


Figure 15. Comparison between microtremor periods and periods from proposed equation

## 6. Conclusions

It was observed that, ranging from complex to simple, there are several types of natural vibration period equations in the literature, and that they all have different period predictions. Considering huge differences in prediction, and organization of the equations available in the literature, which are mainly based on regression analysis, this paper aims at developing a reliable equation including mass and stiffness parameters.

In order to obtain better predictions, microtremor measurements were first taken from 23 RC buildings and their fundamental periods were compared to the dynamic analysis. It was observed that 3D models should be made considering the stiffness contribution of infill walls. While modelling infill walls as equivalent struts, the openings and mass of the infill walls should also be taken into account. It was established that, since infill walls added stiffness to the building, natural vibration periods reduced significantly, and they got closer to the microtremor results.

156 RC buildings were 3D modelled and their dynamic analyses were used to calibrate the proposed equation. The final version of the equation considers the height, principal plan dimensions, load carrying vertical members of the critical storey, and concrete strength of the building. The proposed equation indicates that the period is linearly proportional to the height of the building, nonlinearly proportional to the ratio of the perpendicular plan dimension to plan dimension of the building parallel to the direction considered, and inversely nonlinearly proportional to concrete strength and area of vertical load carrying members.  $H$  is the most effective parameter in the equation because its cubic power affects stiffness of the structure significantly. Following that,  $A_t$  also affects stiffness of the structure but, since it uses plan dimensions of structural elements, its effect is not as significant as that of the height, and its influence rate reduces with the decrease in height. Although  $f_c$  and  $L_j/L_i$  have little influence on the period, they become more effective with an increase in height.

Other than these 156 buildings, 35 different buildings were used in the verification phase and it was observed that the

proposed equation has the lowest error as compared to period equations available in the literature. Besides the overall error, the dispersion of period predictions is also low. The maximum difference of the proposed equation is less than 20 %.

To further understand reliability of the equations, 144 RC building data were collected from the literature and their dynamic analysis results were directly used in the comparison. It was also established that the proposed equation has the lowest error statistics.

Since the proposed equation has better predictions as compared to available equations, it can confidently be utilized in natural vibration period calculations. The equation can predict periods in both principal directions of a typical building. Although the equation has been developed for RC buildings having no more

than 8 storeys, it has been established that it can be utilized for 14 storey buildings as well. As the equation considers concrete strength and the amount of the load carrying members in the direction considered, it can be utilized from frame buildings to shear wall buildings. However, the proposed equation does not consider vertical and plan irregularities. Therefore, it will be possible to add these irregularities to the equation through collection of more irregular building data.

## Acknowledgements

The authors wish to express their sincere appreciation to Van Yuzuncu Yil University (BAP- FYL-2019-8644) for having financed this research program.

## REFERENCES

- [1] Saatcioglu, M., Humar, J.: Dynamic analysis of buildings for earthquake resistant design. *Canadian Journal of Civil Engineering*, 22 (2003), pp. 338-359.
- [2] Asteris, P.G., Repapis, C.C., Repapi, E.V., Cavaleri, L.: Fundamental period of infilled reinforced concrete frame structures. *Structure and Infrastructure Engineering*, 7 (2017), pp. 929-941.
- [3] BSLJ1987.: The Building Standard Law of Japan (BSLJ). Ministry of Construction, Japan, 1987.
- [4] NBCC1995.: National Building Code of Canada. National Research Council of Canada, Canadian Commission on Building and Fire Codes, Canada, 1995.
- [5] UBC97.: Uniform Building Code. Structural Engineering Design Provisions, International Conference of Building Officials. Volume 2. California, 1997.
- [6] TEC2018.: Turkish Earthquake Code. Ministry of Environment and Urbanization, Ankara, Turkey, 2018 (in Turkish)
- [7] Goel, R.K., Chopra, A.K.: Period formulas for moment-resisting frame buildings. *Journal of Structural Engineering*, 123 (1997), pp. 1454-1461.
- [8] Goel, R.K., Chopra, A.K.: Period formulas for shear wall buildings. *Journal of Structural Engineering*, 124 (1998), pp. 426-433.
- [9] Govindan, P., Lakshminpathy, M., Santhakumar, A.R.: Ductility of infilled frames. *Journal of American Concrete Institute*, 83 (1986), pp. 567-576.
- [10] Dowrick, D.J.: *Earthquake Resistant Design for Engineers and Architects*. Second edition. John Wiley & Sons, New York, 1987.
- [11] Negro, P., Verzeletti, G.: Effect of infills on the global behaviour of R/C frames energy considerations from pseudo-dynamic Tests. *Earthquake Engineering and Structural Dynamics*, 25 (1996), pp. 753-773.
- [12] Amanat, K.M., Hoque, E.: A rationale for determining the natural period of R.C. building frames having infill. *Engineering Structures*, 28 (2006), pp. 495-502.
- [13] FEMA356.: *Prestandard and commentary for the seismic rehabilitation of buildings*. American Society of Civil Engineers (ASCE), Federal Emergency Management Agency, Washington DC, 2000.
- [14] ATC-40.: *Seismic evaluation and retrofit of concrete buildings*. Applied Technology Council, Redwood City, 1996.
- [15] Englekirk, R.E., Matthesen, R.B.: Forced vibration of an eight-story reinforced concrete building. *Bulletin of the Seismological Society of America*, 57 (1967) 3, pp. 421-436.
- [16] Trifunac, M.D.: Comparisons between ambient and forced vibration experiments. *Earthquake Engineering and Structural Dynamics*, 1 (1972) 2, pp. 133-150.
- [17] Yu, E., Skolnik, D., Whang, D.H., Wallace, J.W.: Forced vibration testing of a four-story reinforced concrete building utilizing the nees@UCLA mobile field laboratory. *Earthquake Spectra*, 24 (2008) 4, pp. 969-995.
- [18] Beskhyroun, S., Wotherspoon, L., Ma, Q., Popli, B.: Ambient and forced vibration testing of a 13-story reinforced concrete building. In *Proceedings of the New Zealand Society for Earthquake Engineering Conference (NZSEE)*, 2013.
- [19] Soyoz, S., Taciroglu, E., Orakcal, K., Nigbor, R., Skolnik, D., Lus, H., Safak, E.: Ambient and forced vibration testing of a reinforced concrete building before and after its seismic retrofitting. *Journal of Structural Engineering*, 139 (2013) 10, pp. 1741-1752.
- [20] Erdil, B., Tapan, M., Akkaya, İ., Korkut, F.: Effects of Structural Parameters on Seismic Behaviour of Historical Masonry Minaret, *Periodica Polytechnica-Civil Engineering*, 62 (2018), pp. 148-161.
- [21] Akkaya, İ., Özvan, A.: Site characterization in the Van settlement (Eastern Turkey) using surface waves and HVSR microtremor methods, *Journal of Applied Geophysics*, 160 (2019), pp. 157-170.
- [22] Akkaya, İ.: Availability of seismic vulnerability index (K-g) in the assessment of building damage in Van, Eastern Turkey, *Earthquake Engineering and Engineering Vibration*, 19 (2020), pp. 89-204.

- [23] SAP2000.: Structural Analysis Program-2000, Computers and Structures, Inc., v.20.0.0, Berkeley, CA, USA, 2019.
- [24] Chopra, A.K., Goel, R.K.: Building period formulas for estimating seismic displacements. *Earthquake Spectra*, 16 (2000), pp. 33–536.
- [25] Hong, L.L., Hwang, W.L.: Empirical formula for fundamental vibration periods of reinforced concrete buildings in Taiwan. *Earthquake Engineering and Structural Dynamics*, 29 (2000), pp. 327–337.
- [26] Crowley, H., Pinho, R.: Simplified equations for estimating the period of vibration of existing buildings. In *First European Conference on Earthquake Engineering and Sismology*, Geneva, Switzerland, 3–8 September 2006, 1122.
- [27] Guler, K., Yuksel, E., Kocak, A.: Estimation of the fundamental vibration period of existing RC buildings in Turkey Utilizing Ambient Vibration Records, *Journal of Earthquake Engineering*, 12 (2008), pp. 140–150.
- [28] Hatzigeorgiou, G.D., Kanapitsas, G.: Evaluation of fundamental period of low-rise and mid-rise reinforced concrete buildings. *Earthquake Engineering and Structural Dynamics*, 42 (2013), pp. 1599–1616.
- [29] IS2002.: Indian Standard Criteria for Earthquake Resistant Design of Structures Part 1 General Provisions and Buildings (Fifth Revision), Bureau of Indian Standards, New Delhi, 2002.
- [30] Balkaya, C., Kalkan, E.: Estimation of fundamental periods of shear wall dominant building structure. *Earthquake Engineering and Structural Dynamics*, 32 (2003), pp. 985–998.
- [31] Kose, M.M.: Parameters affecting the fundamental period of RC frame with infill walls. *Engineering Structures*, 39 (2009), pp. 93–102.
- [32] Nyarko, H.M., Moric, D., Draganic, H.: New direction based (fundamental) periods of RC frames using genetic algorithms. *15<sup>th</sup> World Conference on Earthquake Engineering (15 WCEE)*, Lisbon, 24–28 September 2012.
- [33] Erdil, B., Ceylan, H.: MVP Interaction Based Seismic Vulnerability Assessment of RC Buildings. *Građevinar* 71 (2019), pp. 489–503.
- [34] Yigit, A.: Elastic Period Calculation Using Structural System Parameters for Low and Medium Height Reinforced Concrete Buildings, Master's Thesis, Van Yuzuncu Yil University, Turkey, 2020 (in Turkish)
- [35] TS498.: Design Load For Buildings, Turkish Standard Institute, Ankara, Turkey, 1987 (in Turkish)
- [36] Polyakov, S.V.: On the interaction between masonry filler walls and enclosing frame when loading in the plane of the wall. Translation in earthquake engineering, *Earthquake Engineering Research Institute (EERI)*, San Francisco, 1960.
- [37] Holmes, M.: Steel frames with brickwork and concrete infilling. In *Proceedings of the Institution of Civil Engineers*, 19 (1961), pp. 473–478.
- [38] Smith, S.B., Carter, C.: A method of analysis for infill frames. In *Proceedings of the Institution of Civil Engineers*, 44 (1969), pp. 31–48.
- [39] Mainstone, R.J.: On the stiffness and strength of infilled frames. In *Proceeding of the Institution of Civil Engineers*, 4 (1971), pp. 57–90.
- [40] Mainstone, R.J., Weeks, G.A.: The influence of bounding frame on the racking stiffness and strength of brick walls. In *Proceedings of the 2<sup>nd</sup> International Brick Masonry Conference*, Building Research Establishment. Watford, England, (1974), pp. 165–171.
- [41] Bazan, B., Meli, R.: Seismic analysis of structures with masonry walls. In *7<sup>th</sup> World Conference on Earthquake Engineering*, International Association of Earthquake Engineering (IAEE), Tokyo, 5 (1980), pp. 633–640.
- [42] Liauw, T.C., Kwan, K.H.: Nonlinear behavior of non-integral infilled frames. *Computers and Structures*, 18 (1984), pp. 551–560.
- [43] Paulay, T., Priestley, M.: Seismic design of reinforced concrete and masonry buildings. John Wiley and Sons, New York, 1992
- [44] Durrani, A.J., Luo, Y.H.: Seismic retrofit of flat-slab buildings with masonry infills. *NCEER Workshop on Seismic Response of Masonry Infills*, San Francisco, California, 4–5 February 1994, pp. 1–8.
- [45] Hendry, A.W.: *Structural Masonry*. Second edition. Macmillan Press, London, 1998.
- [46] Papia, M., Amato, G., Cavaler, i L., Fossetti, M.: Infilled frames influence of vertical load on the equivalent diagonal strut model. In the *14<sup>th</sup> World Conference on Earthquake Engineering*, Beijing, China, 12–17 October 2008, pp. 479–501.
- [47] Bertoldi, S.H., Decanini, L.D., Santini, S., Via, G.: Analytical models in infilled frames. *Proceedings of the 10<sup>th</sup> European Conference in Earthquake Engineering*, Vienna, 28 August–2 September 1994, pp. 1533–1538.
- [48] Ministry of Environment and Urbanization (MEU): The Urban Renewal Law for Regions under Disaster Risk, Law No: 6306, *Official Gazette*, 28309, 52 (2012) (in Turkish).
- [49] Ceylan, H.: Moment, Shear Force and Axial Force (MVP) Interaction Based New Method for Seismic Performance Evaluation of Existing Reinforced Concrete Buildings, Master's Thesis, Van Yuzuncu Yil University, Turkey, 2018 (in Turkish)
- [50] SERU (Structural Engineering Research Unit): Archival Material from Afyon and Bingol Earthquake Database, Middle East Technical University, Ankara, Turkey, August 23, 2017.
- [51] Jennings, P.C., Kuroiwa, J.H.: Vibration and soil-structure interaction tests of a nine-story reinforced concrete building. *Bulletin of the Seismological Society of America*, 58 (1968) 3, pp. 891–916.
- [52] Sozen, M.A.: Lateral drift of reinforced concrete structures subjected to strong ground motion. *Univ. Illinois, Urbana, US*, 1983.
- [53] Elnashai, A.S., Mwafy, A.M.: Overstrength and force reduction factors of multistorey reinforced-concrete buildings. *The Structural Design of Tall Buildings*, 11 (2002) 5, pp. 329–351.
- [54] Burak, B., Comlekoglu, H.G.: Effect of shear wall area to floor area ratio on the seismic behavior of reinforced concrete buildings, *Journal of Structural Engineering*, 139 (2013) 11, pp. 1928–1937.
- [55] Massumi, A., Moshtagh, E.: A new damage index for RC buildings based on variations of nonlinear fundamental period. *The Structural Design of Tall and Special Buildings*, 22 (2013) 1, pp. 50–61.
- [56] Al-Nimry, H., Resheidat, M., Al-Jamal, M.: Ambient vibration testing of low and medium rise infilled RC frame buildings in Jordan. *Soil Dynamics and Earthquake Engineering*, 59 (2014), pp. 21–29.
- [57] Koçak, A.: Prediction of the Fundamental Periods for Infilled RC Frame Buildings. *Karaelmas Science and Engineering Journal*, 7 (2017) 2.
- [58] Aras, F.: Betonarme Binalarda Bölme Duvar Etkilerinin Tam Ölçekli Deneylemlerle Araştırılması. *Teknik Dergi*, 29 (2018) 5, pp. 8651–8668. (in Turkish)